JOURNAL OF MATERIALS SCIENCE 13 (1978) 2659–2670

Microstructural aspects of crack propagation in ceramics

C. Cm. WU,* S. W. FREIMAN,† R. W. RICE, J. J. MECHOLSKY
Naval Research Laboratory, Washington, D.C. 20375, USA

X-ray microradiographic examination supported by optical and SEM observations was used to study crack propagation in various ceramics, including glasses and cubic and non-cubic polycrystalline bodies of different grain sizes. The nature of crack propagation in ceramics was often extremely complex. While cracks in glassy materials were generally simple, as would be expected, in cubic and non-cubic polycrystalline specimens both wandering and branching of cracks was observed. In cubic materials, wandering and branching occurred on the scale of the grain size, while in fine grain, non-cubic materials these were on a multi-grain scale. Results are consistent with the grain size dependence of fracture energy. Elastic anisotropy and thermal expansion anisotropy were suggested as major factors in crack wandering and branching.

1. Introduction

Fracture mechanics measurements based on controlled crack propagation are widely utilized for failure prediction of ceramics. However, details of the nature of these cracks and their microstructural interactions have not been studied. Recently, Mecholsky *et al.* [1] reported that while most ceramics had fracture energies proportional to their elastic modulus, some materials such as partially stabilized ZrO_2, hot pressed Si_3N_4, and graphite fell well above this trend. Microcracking due to thermal expansion anisotropy stresses was postulated as the likely cause of the greater toughness in these materials. This paper reports results of a detailed study of the nature of propagating cracks in ceramic materials. These results generally support the microcracking concept, but also show a wider variety and greater complexity of behaviour.

2. Experimental procedure

The materials of this study are the same or very similar to those that have been extensively used in other studies, e.g. [1], from which characterization data can be obtained. These encompass a variety of commercial and laboratory ceramics, usually having little or no porosity and low, e.g. $< 0.1\%$, impurity levels, but providing a range of grain sizes and mechanical behaviour (see Table I). Double cantilever beam specimens were machined with a groove to guide the propagating crack. The thickness of the specimen underneath the groove was ~ 0.5 mm. The specimens were mounted in a loading fixture (Fig. 1) that could wedge them open to propagate the crack a controlled amount, and be mounted in a modified X-ray microradiography unit.

In the microradiographic unit, a fine grain, high resolution photographic emulsion‡ placed on the back side of the specimen recorded the X-ray beam transmitted in the vicinity of the crack (Fig. 2). The specimen and the recording emulsion were fixed on a stage that allowed them to be translated back and forth together in a direction perpendicular to the incident X-ray beam, so a width of ~ 10 mm or larger could be examined

* Work done while on assignment at the Naval Research Laboratory under Inter-governmental Personnel Act from University of Maryland.

† Present address: Fracture and Deformation Division, National Bureau of Standards, Washington, DC 20234, USA.

‡ Ilford L-4 series and Kodak High Resolution Plates were used with exposure times from a few minutes to a few hours depending on specimen and X-ray parameters.

TABLE I

Materials	Approximate average grain size, G (μm)	Fracture energy γ (J m^{-2})	Primary fracture mode[3]	Separation of crack images, D (μm)[4]	D/G	Sources or processing
(A) Glasses						
Soda-lime glass	N.A.	3.5	N.A.	*	–	PPG Industries
Glassy carbon	N.A.	8.5	N.A.	*	–	Beckwith Carbon Co.
(B) Cubic polycrystals						
ZnSe	50–100	4	T.G.	70–100	1–2	CVD optical grade
$MgAl_2O_3$	150	7	T.G.	40–50	0.3	Sintered, > 99.9%
$MgAl_2O_3$	2	6	T.G.	*	–	dense
MgO	~ 200		T.G. + I.G.	140	0.7	
MgO	50–100		T.G. + I.G.	100	1–2	Hot pressed and annealed
MgO	90	8–12	T.G. + I.G.	70–150	~ 1	> 99% dense
MgO	50		T.G. + I.G.	70	1.4	
MgO	20		T.G. + I.G.	*	–	
ZrO_2 (Y_2O_3 stabilized)	5	13	T.G.	*	–	Hot pressed, 99% dense
SiC(2% B_4C)	100	13	T.G.	(70)	0.7	Ceradyne (hot pressed)
SiC	1–5	18	T.G.	*	–	Norton NC 203 (hot pressed)
(C) Non-cubic polycrystals						
Graphite	5	85[1]	T.G.	50–70	10 ~ 14	POCO Graphite, Inc.
Graphite	75	40–70[1,2]	T.G.	100–140	1.5–2	Union Carbide (ATJ-S)
Al_2O_3	500	23	T.G. + I.G.	700	1.4	Carborundum (Monofrx A) fusion cast
Al_2O_3	100	20	T.G. + I.G.	100–140	1 ~ 1.4	Fusion cast
Al_2O_3	50	~ 40	T.G. + I.G.	140	2.8	Hot pressed and annealed
Al_2O_3	50	32	T.G. + I.G.	~ 70	~ 1.2	General Electric
Al_2O_3	35	22	T.G. + I.G.	~ 70	~ 2	(Lucalox)
Al_2O_3	5	18	T.G. + I.G.	~ 35–70	7–14	
Al_2O_3	2	20	T.G. + I.G.	*	–	Hot pressed
B_4C	70	23	T.G.	~ 200	~ 3	Hot pressed
B_4C	5	23	T.G.	*	–	Hot pressed
MgF_2	0.7	4	T.G.	*	–	Hot pressed optical grade
(D) Two-phase polycrystals						
ZrO_2 (+ 6% Y_2O_3)	0.5	70	T.G.	*	–	Union Carbide (Zircar)
Al_2O_3–ZrO_2	1–10	55	I.G.	~ 70	~ 7	Max Planck Inst.
Li_2O–SiO_2	< 1	100[1]	T.G.	~ 50	~ 50	Crystallized glass
3BaO.5 SiO_2	< 1	17[1]	T.G.	~ 20	~ 20	Crystallized glass
Si_3N_4 (1% MgO)	1	26[1]	I.G.	~ 20	~ 20	Ceradyne (hot pressed)
Si_3N_4 (15% Y_2O_3)	1–2	80[1]	I.G.	~ 70	35–70	Ceradyne (hot pressed)
Si_3N_4	2	12	I.G.	*	–	Reaction sintered

[1] Higher than E–γ trend [1].
[2] Directional dependence.
[3] Fracture mode: T.G. = transgranular; I.G. = Intergranular.
[4] * means no branching or wandering was observed, ( ) indicates primarily wandering.

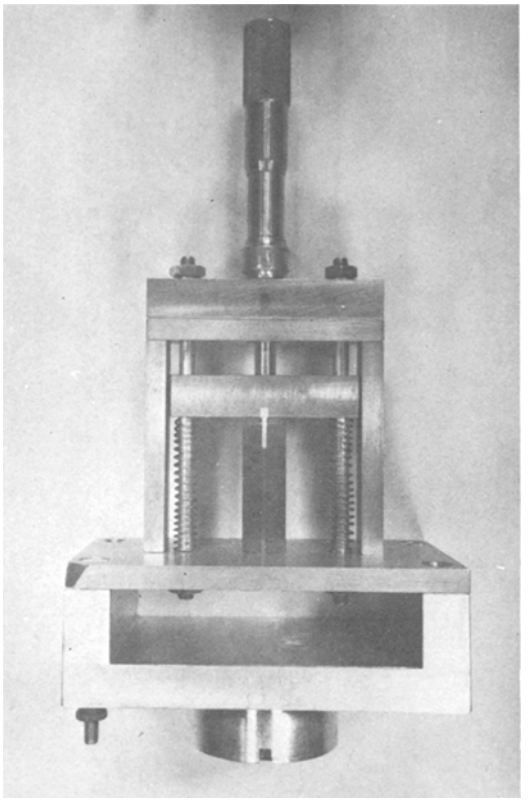

Figure 1 Fixture for fracture and X-ray microradiographic experiment.

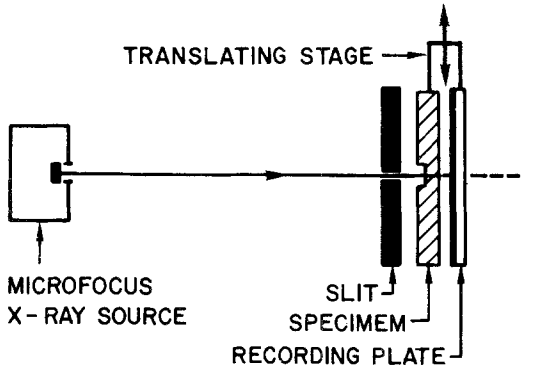

Figure 2 Sketch of experimental set-up.

by a $\sim 150\,\mu$m wide beam. A Lang camera [2] was used so the specimen could also be rotated to any incident angle. An X-ray generator giving a fine spot size ($L \sim 100\,\mu$m square) was used to obtain good resolution since the shortest distance between two points in the specimen that can be resolved is proportional to $L \cdot d/D$ (D = X-ray source to specimen distance and d = specimen to recording emulsion distance). It is impractical to make D too large, since this reduces the X-ray intensity greatly, so it was important to minimize d. Values of $d \sim 0.5$ mm were used, allowing macrocracks a few microns in width to be observed, but isolated microcracks could not be revealed due to the sample thickness which was chosen to be about 0.5 mm as commonly used for fracture energy and crack propagation measurements. Reducing specimen thickness to increase resolution is limited by decreases in contrast differences between cracks and the matrix. Also, if the depth under the groove becomes too thin, effects may become dominated by damage from machining the groove.

The nature of cracks in transparent materials was also examined optically. Post fracture observation of crack propagation surfaces were made by optical and scanning electron microscopy.

Since it was necessary to observe stationary, i.e. arrested cracks, the effects observed are at stress intensities which are unknown fractions of K_{IC}. However, experiments conducted in which microradiographs were obtained after stress removal as well as after re-application of the stresses, indicate no observable difference in crack patterns with applied stress level. Thus while most or all of the cracks near the crack tip closed up so they were beyond resolution with no stress, re-application of the stress resulted in the same or very similar crack pattern. Also, as shown later, results are consistent with experimental and theoretical studies of fracture energy.

3. Results and discussion

Three basic types of crack behaviour were observed in the materials using the microradiographic technique. They are, in order of increasing complexity, twisting, wandering, and branching. These are described in the following three sections. It is important to note that the crack phenomena described in the following sections correlated with grain size and crystal structure regardless of processing or composition, except as specifically noted later.

3.1. Crack twisting

Some crack images were straight bands with occasional varying width along the crack length. This width variation is due to cracks having some twisting as shown by (1) the image of the crack being uniform regardless of its orientation; (2)

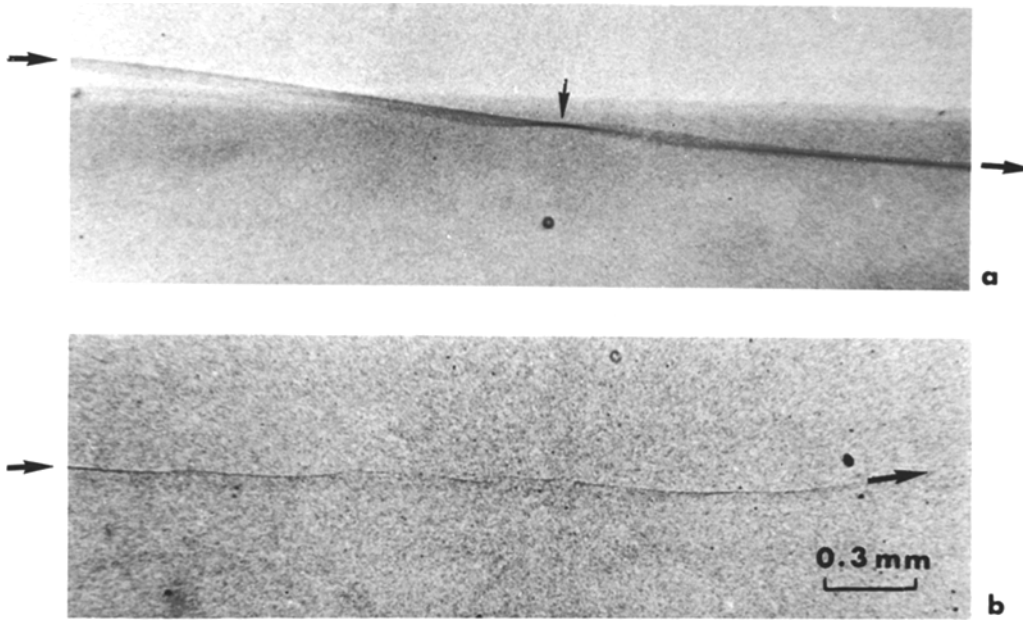

Figure 3 X-ray images of crack in glasses: (a) Soda-lime glass. Note the twisting of the crack surface at point indicated by the smaller arrow. (b) In glassy carbon. Larger horizontal arrows indicate the crack propagation directions; scale mark is for both (a) and (b).

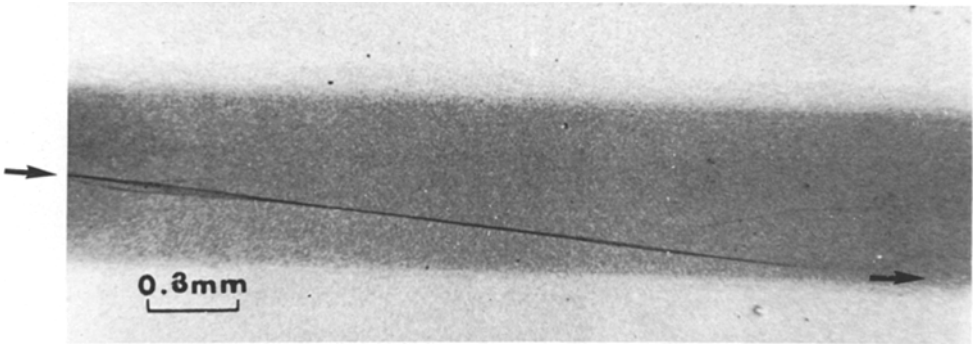

Figure 4 Crack path in fine grain (0.7 μm) MgF_2 showed no branching. Darker central area is crack guiding groove.

rotation of the specimen about the longitudinal axis bringing complete sections of previously broad images into a line image; and (3) direct optical examination, that is, following the crack through the thickness of transparent samples. Twisted cracks were observed in both silicate glasses and glassy carbon (Fig. 3) and in fact, was the only type of phenomena observed in these materials. Crack twisting was also observed in some fine grain polycrystalline materials such as MgF_2 (Fig. 4) where it occurs on a scale very large in comparison to the microstructure. While such sample twisting probably occurs in other polycrystalline materials as well, it is masked by more complex phenomena.

3.2. Crack "wandering"

Many crack images consisted of several generally interwoven, wavy images, (Fig. 5). Based on the following observations, it was determined that most of this waviness was due to the second type of crack behaviour, i.e., a single crack following different paths around or through adjacent grains along the crack front as sketched in Fig. 6; i.e., the crack was a single surface that simply "wandered" on a microstructural scale. First, optical examination of suitably transparent materials, e.g., ZnSe and MgO, showed that as one focused down through the specimens, only one crack was generally present following paths like that sketched in Fig. 6. Second, the waviness was

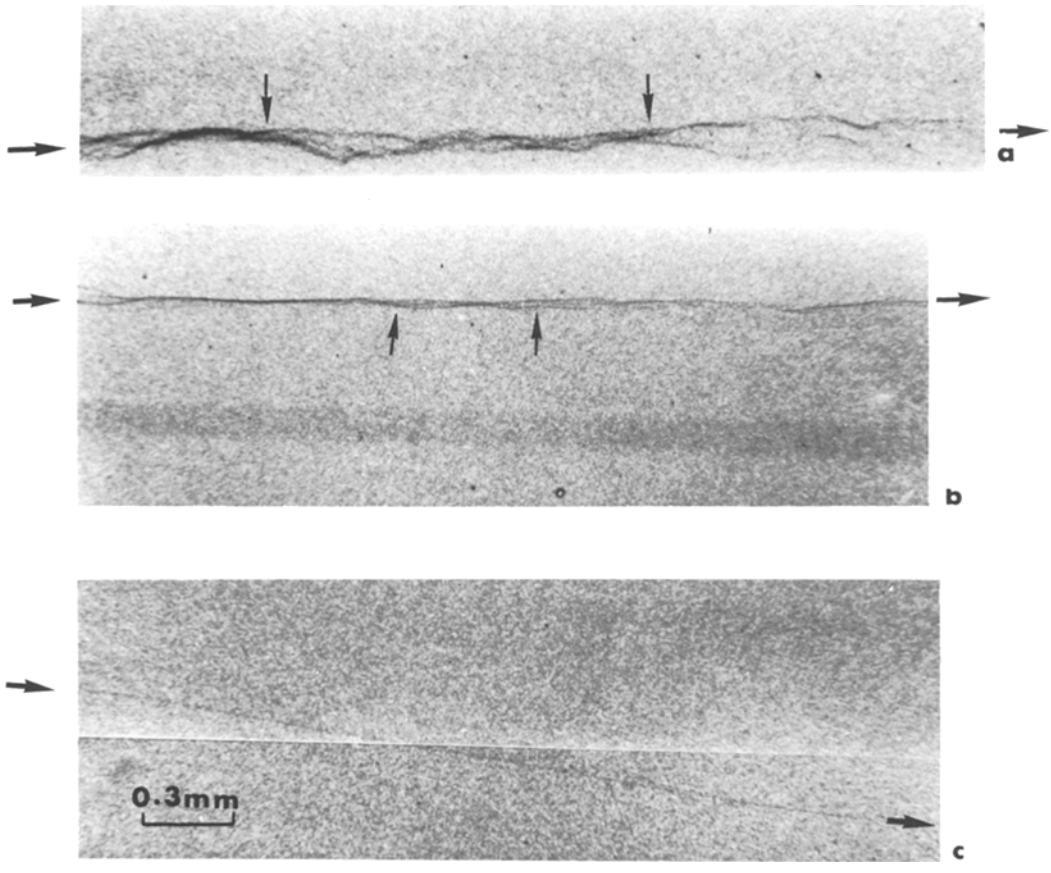

Figure 5 X-ray images of cracks in cubic polycrystalline bodies. (a) Crack "wandering" and branching in large grain (50 to 100 μm) ZnSe. Note also the waviness of crack path. (b) Limited crack branching and "wandering" observed in large grain (150 μm) $MgAl_2O_3$. (c) Fine grain (1 to 5 μm) $MgAl_2O_3$. Note the absence of any apparent branching or "wandering". Small vertical arrows indicate some of the crack "wandering". Larger horizontal arrows indicate crack propagation directions. Scale mark for (a), (b) and (c).

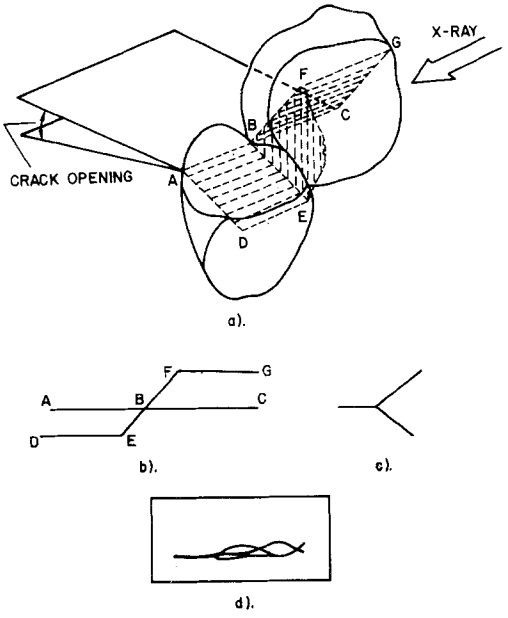

typically from less than 1 grain (due to some transgranular fracture) to only 1 to 2 grains in extent, and individual images were less intense than a complete crack through the thickness. Third, post fracture examination showed the resultant fracture topography correlated with the "wandering". Thus, crack "wandering" is really multiple twisting along the crack front due to interaction with the grain structure. While such "wandering" thus represents a more complex degree of twisting across the crack front, the direct microstructural association of "wandering" and its much greater frequency of occurrence along the crack front distinguish it as a separate phenomena.

Figure 6 Schematic representation of "wandering": (a) local or microstructural view; (b), (c) end and projected view of (a); and (d) resulting X-ray image of crack.

"Wandering" was observed in all cubic polycrystalline bodies with grain sizes larger than about 20 to 30 μm. The absence of observed "wandering" below this grain size range is attributed to resolution limitations. When the specimen is more than ~ 20 grains thick, images due to "wandering" will be superimposed to form a single image band. "Wandering" was also observed in larger grain polycrystalline bodies of non-cubic structure, where it is often complicated by crack branching, which is discussed next.

3.3. Crack branching

The third type of crack behaviour observed was crack branching; i.e., the formation of two or more separate cracks (Figs. 7 to 9). That the observed behaviour is branching and not wandering is shown by: (1) intensities of the separate images being comparable to a single crack; (2) direct optical examination in suitably transparent materials (e.g. ZnSe and MgO); and (3) preliminary studies of crack propagation in SEM. Where branching was observed in fine grain samples, it was on a multi-grain scale, e.g., Figs. 7a, 8b, 9a and b (any branching on the scale of the grain size in such bodies is beyond the resolution of microradiography). Branching in large grain size bodies was on the same scale as wandering (Figs. 7b, 8d and e). Though branching and wandering thus became difficult to distinguish in large grain bodies, study indicates that the extent of branching decreased at larger grain sizes, but that this decrease was approximately balanced by an increase in wandering. In materials showing multi-grain branching in fine grain bodies, the width of the envelope of the branches increased

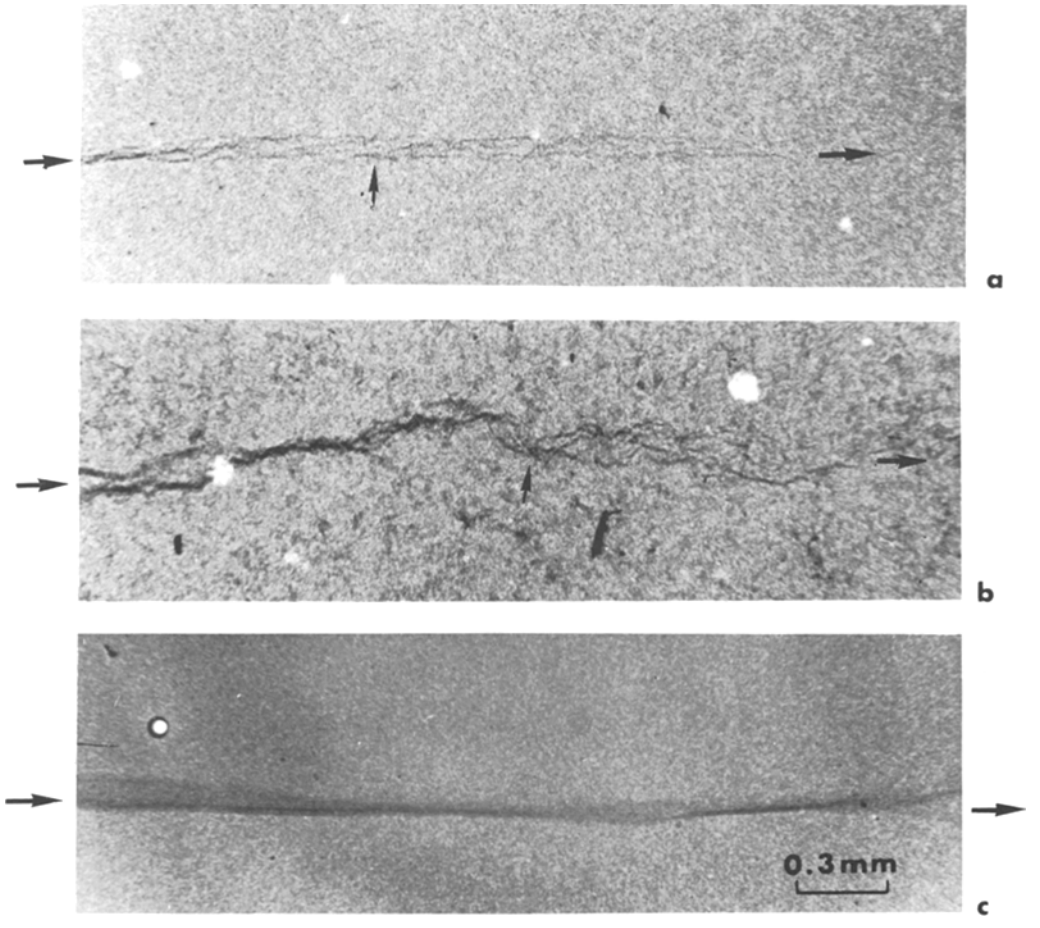

Figure 7 Crack propagation in graphite. (a) Fine (1 to 5 μm) grain POCO graphite; note crack branching as indicated by the smaller vertical arrows. (b) Large (75 μm) grain ATJ-S graphite. Note the crack path appeared to be wavier in ATJ-S than in POCO. (c) Pyrolytic graphite. Note the absence of crack branching. Larger horizontal arrows indicate crack propagation directions. Scale mark for (a), (b) and (c).

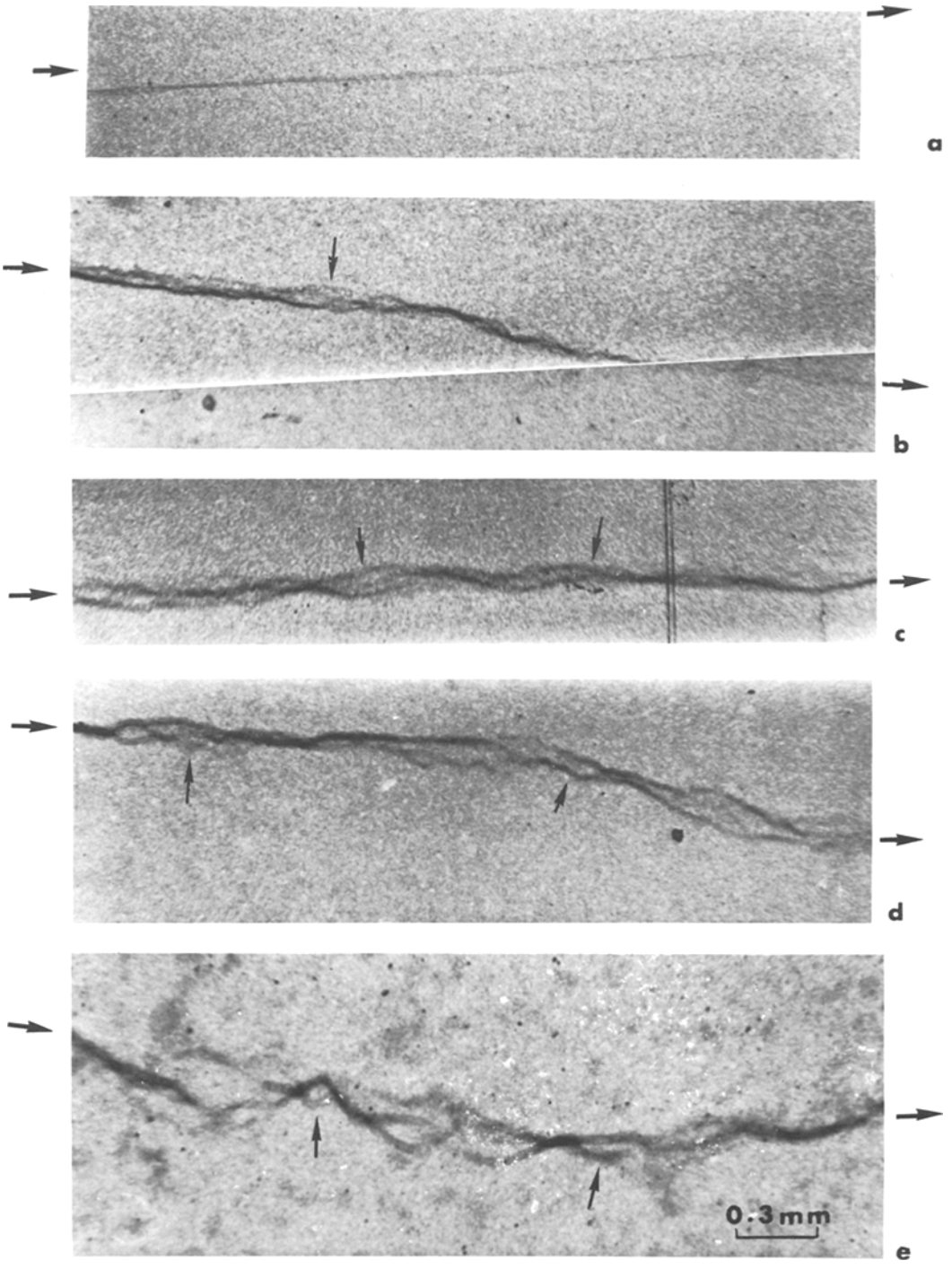

Figure 8 Crack propagation in dense Al_2O_3 of varying grain sizes (G): (a) $G \sim 1\ \mu m$; (b) $G \sim 10\ \mu m$; (c) $G \sim 35\ \mu m$; (d) $G \sim 50\ \mu m$; and (e) $G \sim 200\ \mu m$. The black flecks in (e) are pre-existing microcracks as confirmed by optical microscopy. Note the branching observed in the four larger grain-sized specimens. Larger horizontal arrows indicate crack propagation directions and smaller vertical arrows indicate some of the crack branchings. Scale mark for all five.

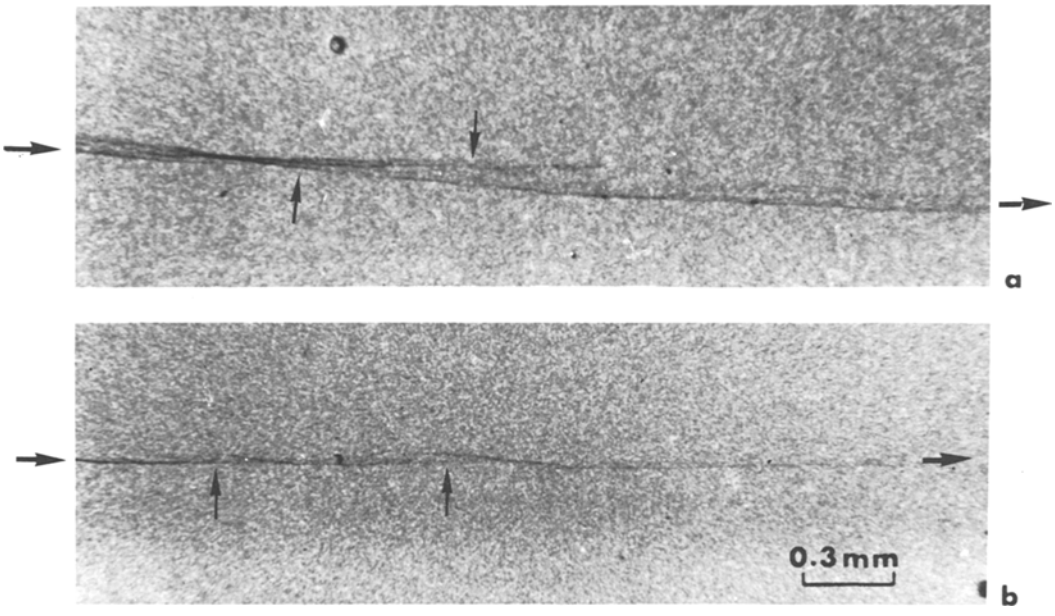

Figure 9 (a) Crack branching observed in hot pressed fine (1 to 5 μm) grain Si_3N_4 + 15% Y_2O_3 and (b) Norton NC-132 Si_3N_4 (1 to 10 μm grain size). Larger horizontal arrows are crack propagation directions and smaller vertical arrows indicate branchings. Scale mark for both (a) and (b).

as grain size increased, but the ratio of the branch separation to the grain size decreased with increasing grain size, especially at large grain sizes, Table I.

Crack branching on a multi-grain scale was observed only in non-cubic or two-phase bodies (Figs. 7 to 9 and Table I). Crack branching on the scale of a few or a single grain scale was observed mostly in large grain non-cubic bodies (no large grain two-phase bodies were available for study) but a limited amount was observed in larger grain cubic materials. Note that in Al_2O_3 where several grain sizes were available, the amount of branching first increased with grain size, i.e., none was seen in the finest grain body and some possible increase of branching occurred with increasing grain size as branching became clearly visible, then levelled off or possibly decreased at large grain sizes. Two other observations should be noted. First, these trends were not determined by processing, e.g. note the overlap in grain size for hot pressed and sintered Al_2O_3. Second, in large grain bodies fracture occurred in part by the linking of pre-existing microcracks along grain boundaries (Fig. 8e). It is shown below that the lack of microcracking in other fine grain non-cubic bodies, e.g., MgF_2, is to be expected in contrast to other bodies exhibiting it.

3.4. Correlation of crack behaviour with fracture energy

The definitiveness of some of the above trends is limited by the number of observations as a function of grain size in any one material. However, the above observations as a function of grain size on any one material as well as isolated observations of one or two grain sizes of other materials are consistent with more extensive theoretical and experimental observations on fracture energy–grain size trends, as are further tests described below. This correlation with fracture energy* behaviour thus provides both coherency and reinforcement of the above trends and suggests the type of phenomena beyond the limits of resolution of microradiography.

Specific crack behaviour–fracture energy correlations are as follows. First, fracture energies of polycrystals are several-fold times single crystal fracture energies. Clearly, the greater fracture area associated with wandering and especially

* Fracture energy data are from [1] or measured by the same constant moment, constant K method. Results are in good agreement with other literature data. Values of E used to calculated values of γ in [1] are standard literature or suppliers' values.

branching (discussed further below) is a significant factor in the increased fracture energy of polycrystals. Propagation of wandering or branching cracks at angles less than 90° to the applied stress may also increase the energy required for fracture. Second, fracture energies of cubic polycrystals have been found to have little or no grain size dependence [3, 4]. This is consistent with wandering being the predominant phenomenon in cubic materials. Since wandering was on the scale of the grain size, the fracture area and hence the fracture energy do not change significantly as grain size changes. This implies that wandering should occur below the resolution of the present study.

Third, the fracture energy of non-cubic polycrystals has been shown to first increase, then pass through a maximum and decrease with increasing grain size [3, 5]. This fracture energy behaviour is consistent with the observed microcracking behaviour. Thus, the increase in branching indicated with increasing grain size in finer grain bodies would increase fracture energies. Correspondingly, the decrease in branching and the increase in cracking by linking pre-existing microcracks at larger grain sizes would decrease fracture energies at large grain sizes.

Fourth, extremely anisotropic bodies such as graphite and some two-phase bodies show fracture energies well above the Young's modulus–fracture energy trends found for most other materials [1]. As shown in Table I, all of these materials showed multi-grain crack branching. The extent of the multi-grain branching also generally correlated with fracture energy, e.g., compare the two hot pressed Si_3N_4 bodies (Fig. 9, Table I). Note that in contrast to these high fracture energy bodies, reaction-sintered Si_3N_4, which has low fracture energy, showed no branching (or discernible wandering, Table I). Further, note that the degree of branching in ATJ-S depended on the relative orientation of the individual specimens with respect to the hot pressing direction and resultant texturing [6]. Thus, more irregular to tortuous branching was observed for cracks growing in the hot pressing direction (perpendicular to most graphite lamellae) in agreement with a higher fracture toughness. Both the more tortuous paths and resultant higher fracture energies are expected because of cracks propagating around the large graphite grains partially oriented so their lamellae tend to be approximately perpendicular to the crack front. On the other hand, no distinct differences in

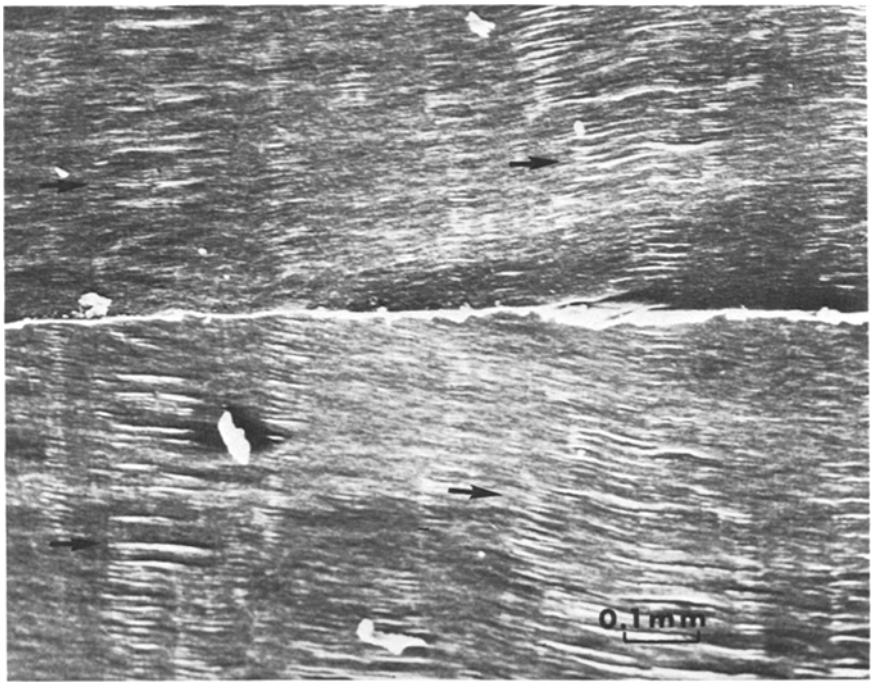

Figure 10 Separation of layers perpendicular to fracture surface observed in pyrolytic graphite. Note, these are matching fracture surfaces.

branching could be observed, in the other two perpendicular orientations as would be expected from their similar texture and fracture energy behaviour [6]. Similarly, pyrolytic graphites showed no branching of cracks propagating perpendicular to the layered structure (Fig. 5c), despite the large grain size (e.g., 50 to 100 μm with layer thickness of about 2.5 μm). On the other hand, optical and SEM examination showed branching due to separation of layers for crack propagation perpendicular to the layered structure (Fig. 10).

3.5. Proposed causes of twisting, wandering and branching

Many materials exhibited far more complex crack propagation than the idealized single, planar crack of most fracture mechanics analysis. Glasses were the only materials consistently approaching this idealized crack behaviour, as expected from their isotropy and the absence of preferred fracture paths. They showed only limited, sporadic twisting which is most likely due to limited material and applied stress variations.

Other crack behaviour was typically substantially more complex, both in its nature and its dependence on material and microstructural parameters. It is not possible at this time to unequivocally explain all of these variations. However, consideration of these results, other results, and basic material properties suggests that elastic anisotropy (EA) and thermal expansion mismatches due to thermal expansion anisotropy (TEA) or between different phases are basic sources respectively of wandering and branching.

Elastic anisotropy, which exists in virtually all crystalline, even cubic, bodies means that the stress distribution around crack tips will vary within, and especially around each grain due to the different elastic strains induced along different grain orientations. Such anisotropy provides a mechanism for crack wandering and is consistent with the observations as discussed below, while other causes that might be considered, e.g. anisotropy of fracture energy appear to have major inconsistencies, such as the fact that wandering occurred with both transgranular and intergranular fracture. Thus, the resultant crack tip stress variations of elastic anisotropy should aid cracks in following different paths either around or through grains for wandering or branching due to sharply differing deflections of nearby portions of the crack front. Further, EA as the mechanism of wandering is generally consistent with it being on the scale of only a few grains because of the rapid drop in stresses away from the crack tip. The limited grain extent of crack wandering is also expected from elastic anisotropy since the applied stress is the only source of strain energy for fracture, failure of a few added grains near the crack reducing energy for further fracture. Some limited crack branching could occur due to EA since different paths around adjacent (or occasionally the same) grains consistent with some limited branching are observed.

The suggested effect of EA is reasonably consistent with the present data and existing measures of EA. Thus, the degree of crack branching as measured by the branch separation to grain size ratio at similar grain sizes (Table I) generally increases as the per cent EA, e.g., as defined by Chung and Bussem [7], increases [A^* (see footnote†): MgO ~ 2.3%, $MgAl_2O_4$ ~ 6.9%, SiC, ~ 7.3%, and ZnSe ~ 11.7%]‡. The possible deviation of MgO from this trend could be due to the occurrence of slip, or the limited, but greater porosity, and possibly greater grain boundary impurity content in it. The use of a more complicated measure of elastic anisotropy as defined by Wachtman [8], while giving the same general trend, changes the relative positions of MgO and $MgAl_2O_4$ and reduces the overall difference (i.e., $MgAl_2O_4 = 0.3$, $MgO = 0.34$, $SiC = 0.34$, and $ZnSe = 0.39$). Quantitatively the trend of the data may be more consistent with this latter measure of anisotropy.

While the above correlations lend support to the suggestions that elastic anisotropy is important, they also show the need for more work. Thus, both the above measures of elastic anisotropy consider elastic constants only along the major crystal axes. A more comprehensive measure of EA, such as a weighted average difference between the single crystal and polycrystalline values over a complete sphere, thus appears necessary. However, the type of average, e.g., based on absolute or r.m.s. differences may be important and needs determination. Similarly, because of data scatter, measurements of bodies having wide ranges of anisotropy, and more

† $A^* = 3(A-1)^2/[3(A-1)^2 + 25A]$, where $A = 2c_{44}/(c_{11} - c_{12})$.
‡ For cubic materials.

closely controlled grain sizes, neither easily obtained, are needed.

Elastic anisotropy, which is typically higher in non-cubic materials, must also be a factor in their behaviour. However, its exact contribution is difficult to assess because of the presence of thermal stresses and because of uncertainties in measuring EA. Not only do the deficiencies of existing measures of EA noted above apply, but non-cubic materials, e.g., Al_2O_3, may not have their maximum or minimum, of either elastic modulus along a principal crystal axis so the existing measures of EA can be quite misleading for non-cubic materials. However, several factors show that thermal expansion differences must be a major factor in the behaviour of non-cubic and two-phase materials.

First, TEA and related stresses are consistent with the multi-grain scale of branching in some non-cubic and two-phase materials. Such stresses are independent of the applied stress, and can be quite large, so they can add to the applied stress, and provide added strain energy to cause more cracking and further from the main or initial crack front. Second, in some of the two-phase materials, there is a much greater difference in the thermal expansion than the elastic properties of the two phases, indicating that stresses from expansion differences are more important. For example, there is less difference in expansion between Si_3N_4 grains [7], than there is between the Si_3N_4 grains ($\alpha \sim 3 \times 10^{-6}\ ^\circ C^{-1}$) and the expected magnesium silicate phases ($\alpha \sim 10 \times 10^{-6}\ ^\circ C^{-1}$), but smaller differences in the Young's moduli (40 to 50×10^6 p.s.i.) of these phases.

Third, the observed results are consistent with recent theoretical results which show mismatch of expansion to be the source of spontaneous cracking in non-cubic bodies [10]. The pre-existing microcracks seen in the large grain Al_2O_3 (Fig. 8e), and reported elsewhere in larger grain crystallized glasses [11], and the Al_2O_3–ZrO_2 body [12] are all consistent with this. Similarly, the increased tendency for intergranular fracture observed in non-cubic materials in this study (Table I) and other studies are consistent with thermal expansion differences at grain boundaries [4].

Fourth, and probably most important, is the fact that recent research shows that thermal expansion differences are the cause of the fracture energy–grain size trend noted earlier for non-cubic materials [3–5]. The fracture energy theory based on TEA not only predicts the observed fracture energy–grain size trends with which the present results are consistent, but also the observed mechanism. Thus, it predicts fracture energy first increasing with increasing grain size due to increased cracking, then decreasing due to more pre-existing microcracks. Further, the latter also provides an explanation for the crack branching and wandering in larger grain non-cubic bodies becoming more on the same scale as the grain size as larger grain sizes are reached. This arises because crack propagation is becoming more a process of linking pre-existing microcracks rather than creating new ones. Since the linking process depends more on the interaction of the stress field around the main crack, microcracks only within a limited distance can be linked up due to the rapid drop of the stress field from the main crack. The increasing reduction of internal stresses and strain energy with increasing generation of pre-existing microcracks at larger grain sizes also increasingly constrains the distance over which branching and wandering can occur. Finally note that the fracture energy theory based on TEA provides an explanation of why the grain size range for multi-grain branching varies. The grain size for any constant degree of cracking is proportional to both the strain mismatch and Young's modulus. Thus for example, the absence of observed branching in MgF_2, despite its greater TEA than Al_2O_3 is consistent with its much lower modulus and finer grain size.

4. Summary and conclusion

There are basic differences in the nature of the crack character in glassy, cubic and non-cubic polycrystalline materials in typical crack propagation tests. In glasses, a single crack having some twist propagates through the sample. In cubic materials, cracks follow differing paths in or around different nearby grains in large grain bodies resulting in the crack surface wandering as it propagates. Wandering is attributed simply to the crack following grain boundaries or cleavage paths at different levels relative to the main crack paths. Elastic anisotropy is suggested as a major cause of wandering in cubic materials. Wandering is expected to occur at all grain sizes, but since it is on the same scale as the grain sizes, it cannot be observed at finer grain sizes due to resolutions limits. Such grain size scaling of

wandering is consistent with the fracture energy of cubic materials showing no significant trend with grain size.

Non-cubic materials, or materials with different grain boundary phases show enhanced crack branching on a multi-grain scale in finer grain bodies. In large grain bodies it occurs on the scale of the grains and some of it becomes crack wandering. Since branching can occur on a multi-grain scale, it represents true changes in fracture area as a function of grain size and generally correlates with changes in fracture energy. These effects generally increase with increasing anisotropy and are consistent with and support the concept of microcracking due to stresses from incompatible strains from thermal expansion anisotropy of the grains or thermal expansion differences between different phases. Thus, the multi-grain scale of wandering and branching in fine grain bodies is attributed to the generation of microcracks around the main crack, while in larger grain bodies, linking of already developed microcracks results in more wandering and less branching, and limiting these to the scale of the grain size.

Acknowledgements

The authors thank Dr P. F. Becher and Dr W. J. McDonough for helpful discussions during the course of the investigations. We also thank Mr C. Vold for the use of X-ray facilities and P. C. Miller for assistance in the construction of the loading fixture. C. Cm. Wu is very grateful to the Naval Research Laboratory, especially Mr R. W. Rice, for the opportunity to participate in this project through the IPA Program.

References

1. J. J. MECHOLSKY, S. W. FREIMAN and R. W. RICE, *J. Mater Sci.* **11** (1976) 1310.
2. A. R. LANG, *Acta Cryst.* **12** (1959) 249.
3. R. W. RICE and S. W. FREIMAN, submitted to *J. Amer. Ceram. Soc.*
4. R. W. RICE, "Treatise in Materials Science", Vol. II, edited by R. K. MacCrone (Academic Press, New York, 1977) p. 199.
5. R. W. RICE, S. W. FREIMAN, R. C. POHANKA, J. J. MECHOLSKY Jr and C. Cm. WU, presented in Symposium on the Fracture Mechanics of Ceramics, Penn State University, 1977 (to be published).
6. C. Cm. WU, S. W. FREIMAN and J. J. MECHOLSKY, Reentry Vehicle Materials Technology (Remat) Program: Fracture Mechanics of Graphite and C-C Composites, NRL-0087-5, Naval Research Laboratory, Washington, DC (1975), p. 18.
7. D. H. CHUNG and W. R. BUESSEN, "Anisotropy in Single Crystal Refractory Compounds", edited by F. W. Vahldiek and S. W. Mersol, (Plenum Press, New York, 1968 p. 217.
8. J. B. WACHTMAN Jr, "Fracture Mechanics, Vol. 1, edited by R. C. Bradt, D. P. H. Hasselman and F. F. Lange, (Plenum Press, New York, 1974) p. 49.
9. C. M. B. HANDERSON and D. TAYLOR, *Trans. J. Brit. Ceram. Soc.* 74 (1975) 49.
10. R. W. RICE and R. C. POHANKA, submitted to *J. Amer. Ceram. Soc.*
11. S. W. FREIMAN and L. L. HENCH, *J. Amer. Ceram. Soc.* 55 (1972) 86.
12. N. CLAUSSEN, *ibid.* 59 (1976) 49.

Received 25 October 1977 and accepted 9 March 1978.